Nonlinear adaptive filters for high-speed LED based underwater visible light communication [Invited]

Nan Chi (迟 楠)* and Fangchen Hu (胡昉辰)

Shanghai Institute for Advanced Communication and Data Science, Key Laboratory for Information Science of Electromagnetic Waves (MoE), Fudan University, Shanghai 200433, China

**Corresponding author: nanchi@fudan.edu.cn*

Received August 25, 2019; accepted September 12, 2019; posted online October 15, 2019

Underwater visible light communication (UVLC) is expected to act as an alternative candidate in next-generation underwater 5G wireless optical communications. To realize high-speed UVLC, the challenge is the absorption, scattering, and turbulence of a water medium and the nonlinear response from imperfect optoelectronic devices that can bring large attenuations and a nonlinearity penalty. Nonlinear adaptive filters are commonly used in optical communication to compensate for nonlinearity. In this paper, we compare a recursive least square (RLS)-based Volterra filter, a least mean square (LMS)-based digital polynomial filter, and an LMS-based Volterra filter in terms of performance and computational complexity in underwater visible light communication. We experimentally demonstrate 2.325 Gb/s transmission through 1.2 m of water with a commercial blue light-emitting diode. Our goal is to assist the readers in refining the motivation, structure, performance, and cost of powerful nonlinear adaptive filters in the context of future underwater visible light communication in order to tap into hitherto unexplored applications and services.

OCIS codes: 060.4510, 070.4340, 120.2440.

doi: 10.3788/COL201917.100011.

With the development of modern technologies, human's activities are gradually extended to the underwater environment from land. Lots of activities urgently need reliable, convenient, and high-capacity communication in the underwater environment instead, such as environmental monitoring, underwater exploration, and aquaculture[1]. Consequently, underwater communication technology has attracted special interest of researchers worldwide. Due to the advantages of cost-effective, license-free immunity to electromagnetic interference and high security, visible light communication (VLC) is an alternative candidate in next-generation underwater wireless optical communications (UWOCs)[2–5]. Compared with existing technology such as bluetooth or wireless LAN (802.11), VLC has a much lower attenuation in water for high-frequency radio[4]. One way around this is using ultra-low frequency long-wave radio, for which the attenuation is manageable, but the maximum bandwidth is significantly limited. Sonar communication is another possibility, but available modems and transducers are too large and very expensive. Exploiting the low absorption window of seawater in the blue-green portion of the electromagnetic spectrum, VLC is expected to play an important role by offering secure, efficient, and high data rate communications among submarines, unmanned underwater vehicles, ships, divers, buoys, and underwater sensors within a short range (<100 m). In addition, UWOC can be utilized to investigate climate change as well as monitor ecological and biogeochemical changes in the ocean, sea, and lake environments[6]. In underwater visible light communication (UVLC), both a laser diode (LD) and a light-emitting diode (LED) can be used as a transmitter. Many results about beyond the Gbit rate have been published utilizing LDs[7–9] while for LEDs only 161.1 Mb/s over 2 m[10] and 800 Mb/s over 0.6 m[11] are experimentally demonstrated. Besides, the cost of LEDs is much lower than that of LDs, and LDs may cause safety issues such as damaging human eyes.

However, UVLC still faces many problems. First is the absorption, scattering, and turbulence[3,12]. Absorption is the irreversible loss of power as light propagates in the medium. Scattering refers to the deflection of light from its original path. On the microscopic level, scattering corresponds to the interaction between a photon and a molecule or an atom. Particles with different shapes, types, and concentrations effectively determine the scattering properties of the medium. The performance of a UVLC system can also be affected by channel fading as a result of oceanic turbulence. This is similar to the atmospheric turbulence in free-space optical communication[13]. Blobs of turbulent waters of different sizes can slightly and continuously change the propagation direction of photons due to the variation of the index of refraction of the medium. All of these effects will result in both amplitude and phase distortion for the output signal of the UVLC system[13]. Another one is the nonlinear effect derived from the nonlinear electro-optic conversion of the LED[3], the square-law detection and saturation effect of the photodiode (PD)[14], and the nonlinear response of electrical devices, e.g., electronic amplifiers[15]. To systematically illustrate the nonlinear effect existing in our UVLC system, an amplitude–amplitude (AM–AM) curve of the input signal and output signal, the S21 parameters of the VLC system are given in Fig. 1. The AM–AM curve (left figure in Fig. 1) shows the obvious nonlinearity of

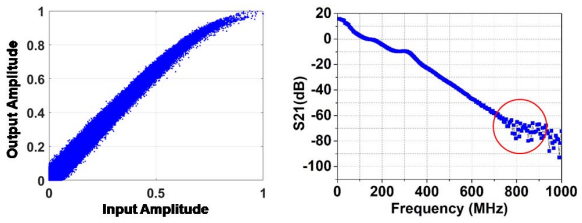

Fig. 1. Nonlinear response of the UVLC system in the time domain and frequency domain.

the system response when the amplitude of the input signal is high. Such nonlinearity mainly comes from the limitation of the LED and PD mentioned above. Besides, the value of the S21 parameter decreases with the increase of the frequency (right figure in Fig. 1), indicating that the underwater channel is a strongly fading channel. The uneven response in the high-frequency range (circled by a red circle) also validates the existence of nonlinear effects resulting from the limits of the device bandwidth. For further understanding the linear and nonlinear distortion from the UVLC channel, a specific channel model considering both underwater conditions and device limitation is provided[3] as follows:

$$H(w) = H_t(w) \cdot H_c(w) \cdot H_r(w), \tag{1}$$

$$H_c(w) \approx 10\log_{10}\left[\left(\frac{D_R}{\theta_{1/e}d}\right)^2 e^{(a+b)d\left(\frac{D_R}{\theta_{1/e}d}\right)^T}\right]. \tag{2}$$

In Eq. (1), the complete system function $H(w)$ is obtained by the multiplication of $H_t(w)$, $H_c(w)$, and $H_r(w)$ in order, which respectively stand for the system function of the transmitter, underwater channel, and receiver part. Specifically, $H_t(w)$ and $H_r(w)$ mainly depend on the characteristics of the LEDs and PDs described on their device data sheets, and additionally the nonlinear effect is included. As for the underwater channel system function $H_c(w)$, a path loss channel model of Eq. (2) was proposed according to the Beer–Lambert formula by M. Elamassie in 2018. This equation is determined by the parameters a and b, which respectively denote the absorption and scattering coefficients. The rest of the parameters are referenced in Ref. [16]. If the influence of turbulence for UVLC is also added, the gamma–gamma turbulence model is provided, revealing the random intensity and phase fluctuations and impaired link performance for the received signal[17,18].

In order to comprehensively compensate such linear and nonlinear impairments from the underwater channel and VLC devices, adaptive nonlinear filters are proposed to apply in UVLC. In this paper, three nonlinear adaptive filters [a recursive least square (RLS)-based Volterra filter, a least mean square (LMS)-based digital polynomial (DP) filter, and an LMS-based Volterra filter] are used to mitigate the effects of scattering, absorption, turbulence, and devices. We want to show the performance of different nonlinear equalizations in UVLC in order to provide a reliable reference for future researchers. In addition, 2.325 Gb/s UVLC transmission is experimentally demonstrated at a distance of 1.2 m with a commercial blue LED.

RLS and LMS are two classic adaptive filter algorithms. RLS recursively finds the coefficients that minimize a weighted least squares cost function relating to the input signals[19] while LMS mimics a desired filter by finding the filter coefficients that relate to producing the LMS of the error signal. For linear filters, RLS exhibits extremely fast convergence and low mean square error at the cost of high computational complexity compared with LMS.

A Volterra-series-based equalizer appears to be a good choice for the nonlinear effect. Volterra series can be used to simultaneously estimate the response of a nonlinear system and capture the memory effect of devices or water[20]. The DP-based equalizer is another simplified nonlinear filter that is usually used as digital pre-distortion[21], but also works as post equalization. In this section, we want to describe three nonlinear adaptive filters: RLS-based Volterra filter, LMS-based DP filter, and LMS-based Volterra filter.

Figure 2 shows the schematic diagram of an RLS-based Volterra filter. Considering the trade-off between computation complexity and equalization performance, only the first-order and second-order terms of the Volterra series are used in the calculation. The first-order term is the linear part of the signal, while the memory length is N. The second-order term is the combination of different delayed signals. So, the input sequence of the RLS filter is described as

$$\begin{aligned} x(n) &= x_l(n) + x_{nl}(n) \\ &= \sum_{l_1=0}^{N} w_{l_1}(n)x(n-l_1) \\ &\quad + \sum_{l_1=0}^{N}\sum_{l_2=0}^{N} w_{l_1,l_2}(n)x(n-l_1)x(n-l_2), \end{aligned} \tag{3}$$

where $x_l(n)$ are the linear outputs of the Volterra series. $x_{nl}(n)$ is the nonlinear output of the Volterra series. $w_{l_1}(n)$ and $w_{l_1,l_2}(n)$ are the weight coefficient sequences of the first-order and second-order terms of the Volterra series. Equation (3) applies to Figs. 2 and 4. Training sequences

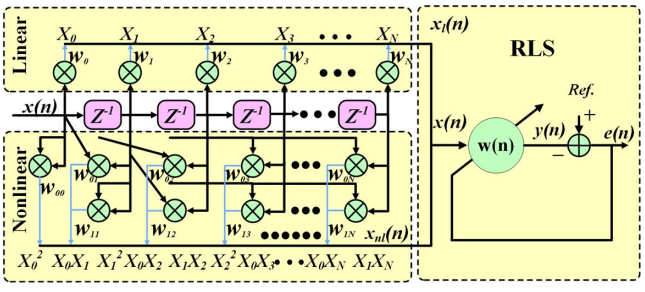

Fig. 2. Schematic diagram of the RLS-based Volterra filter.

are used to update the weight coefficients according to the RLS error function expressed as

$$\xi^d(n) = \sum_{i=0}^{n} \lambda^{n-i} \varepsilon^2(i) = \sum_{i=0}^{n} \lambda^{n-i} \big[d(i) - x^T(i) w(n)\big]^2, \tag{4}$$

where ε signifies the posterior error and is related to the transmitted symbol d at time i, the received signal x at time i, and the weight coefficient sequence w of the current time. λ is the forgetting factor to achieve convergence of the error function.

Figure 3 shows the schematic diagram of the LMS-based DP filter. It is a much simpler structure than the Volterra filter. The output sequence of the DP filter is as follows:

$$\begin{aligned} x(n) &= x_l(n) + x_{nl}(n) \\ &= \sum_{l_1=0}^{N} w_{l_1}(n) x(n - l_1) \\ &\quad + \sum_{l_1=0}^{N} w_{l_1,l_1}(n) x(n - l_1) x(n - l_1). \end{aligned} \tag{5}$$

Only quadratic terms of different delayed signals are considered. The cross terms are omitted to reduce the computational complexity. Training sequences are used to update the weight coefficients according to the LMS error function. In Fig. 3, u is an adjustable parameter for the convergence of the LMS.

Figure 4 shows the schematic diagram of the LMS-based Volterra filter. The structure is the same as that of the RLS-based Volterra filter, except the update algorithm. The weight coefficients are updated by the LMS algorithm. The LMS error function is shown as

$$e^2(n) = \big[d(n) - x^T(n) w(n)\big]^2, \tag{6}$$

where $e(n)$ is the prior error and is related to the transmitted signal $d(n)$, received signal $x(n)$, and weight coefficient sequence $w(n)$ at current time n. The error function of the LMS is the squared estimate of the instantaneous error, which is different from the RLS at this point.

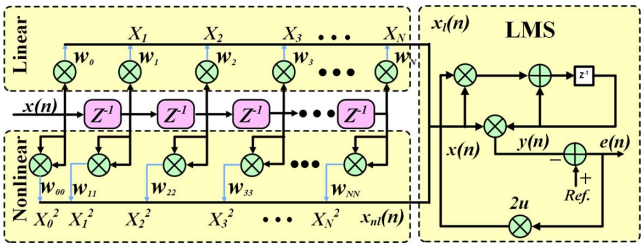

Fig. 3. Schematic diagram of the LMS-based DP filter.

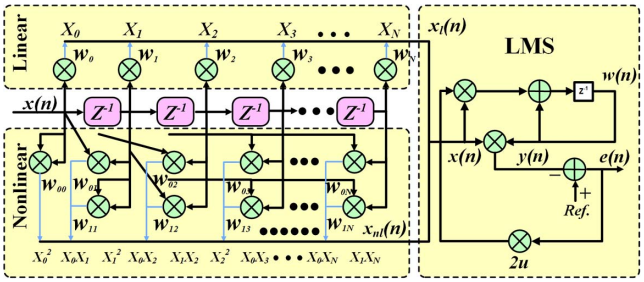

Fig. 4. Schematic diagram of the LMS-based Volterra filter.

Next, we discuss the computational complexity of three nonlinear adaptive filters. Considering the chip resource and power consumption of digital signal processing in application specific integrated circuits, the cost of a multiplier is much higher than that of an adder. Therefore, computational complexity of those filters is evaluated in terms of the number of multipliers per bit. The detailed computational complexity of these three equalizers is shown in Table 1. N_{linear} is the tap number of the linear part, $N_{\text{nonlinear}}$ is the tap number of the nonlinear part. Usually, computational complexity includes two parts, the output part and update part. The structure of the filter determines the output part, while the update part relies on the update algorithm.

According to the table, it is clear to see that RLS has a much larger computational complexity than LMS, while the DP filter is simpler than the Volterra filter. For simple comparison, we set the linear tap length equal to the nonlinear tap length. Figure 5 shows the computational complexity of three nonlinear equalizers. As the RLS-based Volterra filter has a too large number of multipliers, we have to use a logarithm to show the difference between the three methods.

Figure 6 shows the block diagrams of the UVLC single input multiple output (SIMO) system. Such an SIMO system is a spatial diversity transceiver using power multiplexing to mitigate the deep fading caused by complex underwater conditions. This spatial system has a verified signal-to-noise ratio (SNR) reduction of more than 15 dB compared to the SISO system[22]. As a result, an SIMO system is proposed for underwater 5G application and is utilized as our experimental setup in this Letter to meet the urgent demand for high accuracy and capacity.

First, we generate the drive signal by the AWG with an offline MATLAB® program. A hardware pre-equalization circuit is applied to compensate the channel response. Before coupling with direct current by Bias Tee, the signal is amplified by an electrical amplifier (EA). A commercial blue LED is used as the transmitter in the experiment. Then, a lens is placed after the LED in order to emit parallel light into the water. The length of the water tank is 1.2 m. At the receiver side, two differential receivers are used after two lenses focusing the light. The differential receiver consists of a PIN, a transimpedance amplifier (TIA), and a differential circuit. Finally, the signals

Table 1. Computational Complexity

Algorithm	Output	Update
RLS–Volterra	$N_{\text{linear}} + \frac{N_{\text{nonlinear}}(N_{\text{nonlinear}}+1)}{2} \cdot 2$	$4N_{\text{linear}} + 3{N_{\text{linear}}}^2 + 3N_{\text{linear}}N_{\text{nonlinear}} + 6N_{\text{linear}}{N_{\text{nonlinear}}}^2 + 6N_{\text{linear}}{N_{\text{nonlinear}}}^3 + 6N_{\text{linear}}{N_{\text{nonlinear}}}^4 + 4{N_{\text{linear}}}^3 + 6{N_{\text{linear}}}^2N_{\text{nonlinear}} + 6{N_{\text{linear}}}^2{N_{\text{nonlinear}}}^2 + 2N_{\text{nonlinear}} + \frac{11}{4}{N_{\text{nonlinear}}}^2 + 2{N_{\text{nonlinear}}}^3 + \frac{9}{4}{N_{\text{nonlinear}}}^4 + \frac{3}{2}{N_{\text{nonlinear}}}^5 + \frac{1}{2}{N_{\text{nonlinear}}}^6$
LMS–DP	$N_{\text{linear}} + N_{\text{nonlinear}} \cdot 2$	$N_{\text{linear}} + 1 + N_{\text{nonlinear}} + 1$
LMS–Volterra	$N_{\text{linear}} + \frac{N_{\text{nonlinear}}(N_{\text{nonlinear}}+1)}{2} \cdot 2$	$N_{\text{linear}} + 1 + \frac{N_{\text{nonlinear}}(N_{\text{nonlinear}}+1)}{2} + 1$

Note: N_{linear} is the tap number of the linear part and $N_{\text{nonlinear}}$ is the tap number of the nonlinear part.

are sampled by a digital real-time oscilloscope with a 5 GSa/s sampling rate.

At the transmitter side, the signal is modulated by 64-QAM discrete multi-tone (DMT) modulation. While in the offline process of the receiver, two data streams are first combined using the maximal-ratio combining (MRC) algorithm. Before DMT demodulation, a nonlinear compensation algorithm is used to mitigate the effect of water transmission. In this paper, one RLS-based Volterra filter, an LMS-based DP filter, and an LMS-based Volterra filter are utilized as nonlinear equalization.

First, we measured the BER performance with different bandwidths in the UVLC system when choosing different numbers of adaptive filter taps. The results are presented in Fig. 7. While BER is below the threshold of 3.8×10^{-3} with 7% forward error correction (FEC), the system can be viewed as zero-error communication and the operation range is drawm by a black line. For all three nonlinear adaptive filters, when the number of taps is fixed and the bandwidth of the signal is increasing, the BER will rise because the limited number of taps constrains the equalization performance of the filters. If the number of taps is not enough, some linear and nonlinear damage induced by interference between different symbols cannot be compensated completely. As a result, the transmission quality will decrease. Overall, when the bandwidth is higher, it is observed that the performance of the system becomes better as the number of taps increases. However, the BER will stop reducing when the number of taps is enough but continues increasing. This is because the interference only occurs between a limited number of symbols.

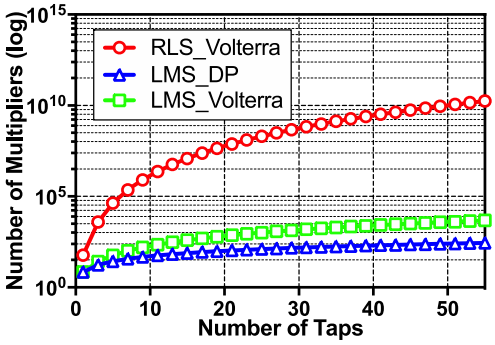

Fig. 5. Computational complexity versus number of taps.

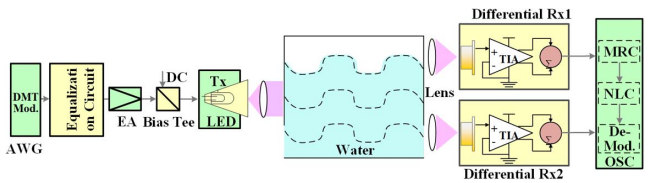

Fig. 6. Block diagram of the UVLC system.

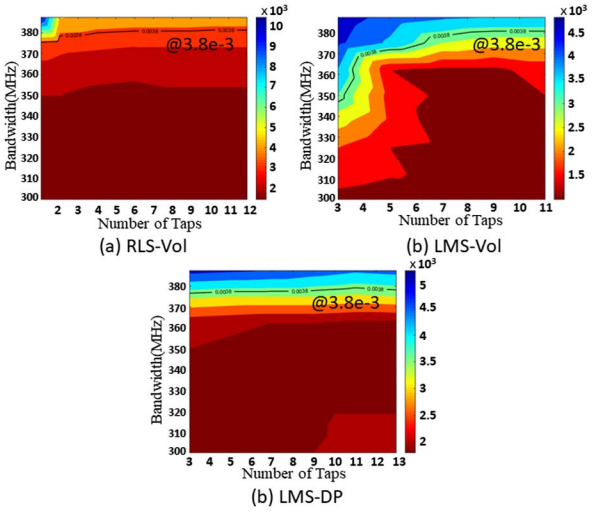

Fig. 7. BER performance versus bandwidth and number of taps for different nonlinear adaptive filters in the UVLC system.

If the number of taps exceeds the value of it, the performance of the filter will not be further improved.

Under the optimal taps of the filter, we measured the time-domain wave of the transmitted signal and received signal after equalization. The blue and red lines in Fig. 8 represent the time-domain wave of the transmitted and received signals, respectively. The results show that the amplitude of the waveform of the received signal can be compensated successfully through all of nonlinear adaptive filters. In addition, it is also found that RLS–Volterra is a relatively better nonlinear filter and the waveform of the signal after its equalization is smoother and more closely matches the waveform of the transmitted signal than LMS–Volterra and LMS–DP. According to the ignorance of the cross term of the training sequence, the nonlinear-resistance of LMS–DP is the worst and the equalized signal is a little more uneven than the others. This phenomenon can be observed from the area in the black circle. The constellation also clearly shows their equalization performance.

A nonlinear adaptive filter's function is not only reflected from the time domain, but also indicated from the frequency domain. As we all know, the frequency response of VLC channel will suffer serious high-frequency attenuation. Figure 9(b) shows obvious high-frequency attenuation and nonlinear effects. Nonlinear damage makes the signal frequency spectrum no longer smooth compared to the transmitted signal in Figs. 9(a).

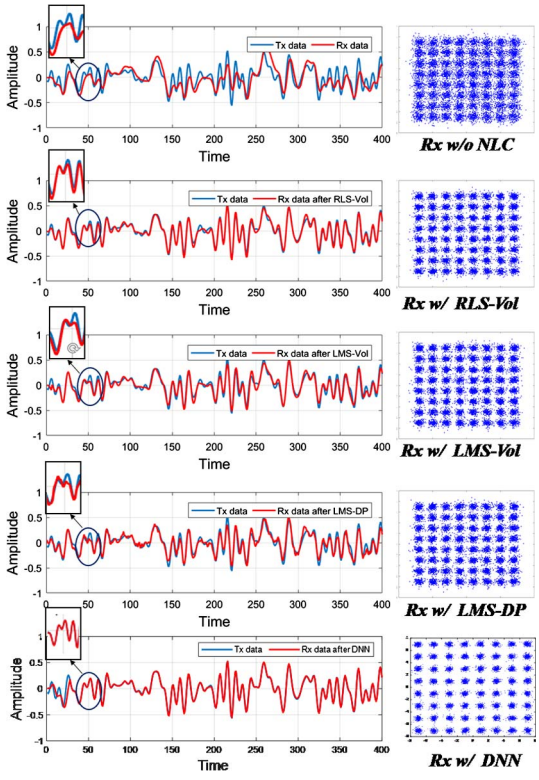

Fig. 8. Time-domain waveform comparison of the transmitted signal and received signal after the nonlinear adaptive filter and the DNN proposed by Ref. [3].

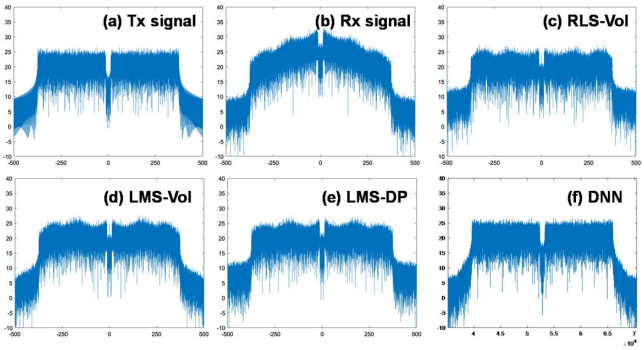

Fig. 9. Spectral response of (a) transmitted signal, (b) received signal without nonlinear equalization, (c) signal with RLS–Volterra nonlinear equalization, (d) signal with LMS–Volterra nonlinear equalization, (e) signal with LMS–DP nonlinear equalization, and (f) signal with the DNN proposed by Ref. [3].

Figures 9(c), 9(d), and 9(e) are the spectral responses of the signal after different filters. In general, the amplitude of the spectral response becomes similar to that of the transmitted signal. However, it is not as smooth as the transmitted signal because the order of Volterra and DP is only second order, which limits the performance of nonlinear equalization.

Without considering cross terms of symbols, LMS–DP is expected to be the worst filter for nonlinear equalization. However, what is the performance comparison between LMS–Volterra and RLS–Volterra? First, we compared the error convergence speed of RLS–Volterra and LMS–Volterra in Fig. 10. RLS is an algorithm that recursively finds the filter coefficients. LMS is an algorithm that uses the gradient descent method. Each time filter coefficients are updated, the computational complexity of RLS is much larger than that of LMS. That is to say, it converges exponentially and faster than LMS. LMS's convergence speed and performance are much related to step size and gradient descent method. If we choose a suitable step size, the equalization performance is optimal, but the convergence speed is relatively slow. From Fig. 11, it is obvious that RLS has a faster convergence speed, which has already converged when the number of training samples is 200. However, LMS converges when the number of training samples is around 2000.

To evaluate the performance of different nonlinear equalizations in water, we also test the performance of

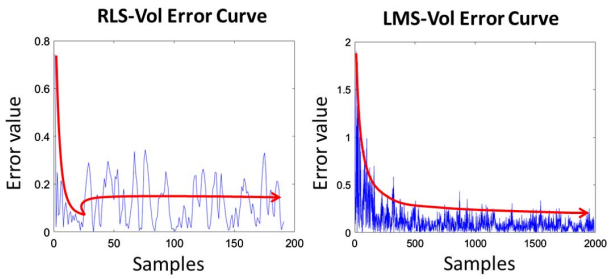

Fig. 10. Error convergence curve of the RLS–Volterra and LMS–Volterra filters.

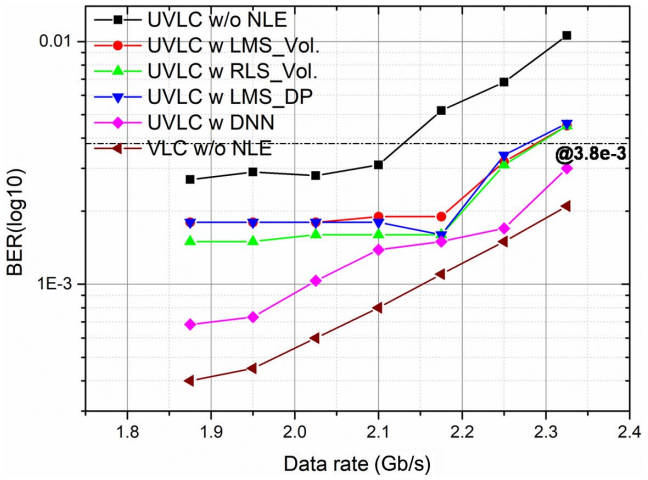

Fig. 11. BER versus bandwidth for the VLC and UVLC systems.

VLC, where the transmission medium is air. The result is shown in Fig. 11. The orange dash line indicates the great BER performance of this system over 1.2 m air. The black line indicates the poor performance of UVLC over 1.2 m water without any nonlinear equalizations. Comparing these two situations, it is clear to see that the water medium can bring a great penalty compared with the air medium. The red, blue, and green lines are, respectively, the performance of UVLC after the RLS-based Volterra filter, the LMS-based DP filter, and the LMS-based Volterra filter. 2.325 Gb/s UVLC transmission is experimentally demonstrated under the hard-decision forward-error-correction (HD-FEC) threshold at a distance of 1.2 m with a commercial blue LED. There is a slight difference between these three methods. Overall, the RLS-based Volterra filter and LMS-based Volterra filter almost have the same performance, and they are both a little better than the LMS-based DP filter. However, considering the computational complexity, the LMS-based DP filter is the lowest one, while RLS is the highest one. The enhancement of the performance is not obvious mainly because the order of the Volterra is only 2 and nonlinear effect cannot be completely compensated when nonlinearity is serious. But a higher-order nonlinear effect does exist in the VLC system[23]. If the computation ability is improved when staging into 5G, a higher-order Volterra filter or deep neural network (DNN) filter could be successfully applied and further enhance the performance of UVLC systems[3].

In addition to the attenuation introduced by scattering and turbulence of water, the irreversible loss of power as light propagates in the medium is also a serious problem. From the figure we can see that, as the bandwidth decreases, the performance of the UVLC system is not further improved. This is totally different from the result in air. The SNR of the UVLC system is limited by the absorption and transmission distance.

In this paper, 2.325 Gb/s UVLC transmission is experimentally demonstrated at a distance of 1.2 m with a commercial blue LED employing a nonlinear adaptive filter. RLS-based Volterra filter, LMS-based DP filter, and LMS based Volterra filter are all achieved and compared in this paper in terms of BER performance and computational complexity. According to our results, the RLS-based Volterra filter and LMS-based Volterra filter almost have the same performance, and they are both a little better than the LMS-based DP filter. However, the LMS-based DP filter has the lowest computational complexity while RLS has the highest one. Considering the trade-off between computation complexity and equalization performance, the LMS-based DP filter and LMS–Volterra filter appear to be more practical algorithms to mitigate the attenuation and nonlinearity introduced by scattering, turbulence of water, and devices. Recently, a DNN-based UVLC system has been proposed and demonstrated in Ref. [3]. We also compare the BER performance of DNN and nonlinear adaptive filters in this Letter. The results show that DNN performs better than all of these filters because of its superior ability for regression problems[24]. Most of the linear and nonlinear distortion is successfully mitigated as observed from the satisfactory time-domain waveform and frequency spectrum of the equalized signal by DNN in Figs. 8 and 9. However, it is still hardly proposed for the application scenarios with a strict demand for latency and cost due to its huge computation complexity[25]. Consequently, there is a trade-off between computation complexity and performance needing to be considered in practical complement.

For future research in underwater VLC, the absorption of water is a breakthrough point if we can further improve the optical focusing system. Besides, seawater in suspension and dissolved particles is a more urgent and practical issue. Ocean, which is significant for both industry and military areas, covers about more than 2/3 surface on the Earth. We believe that UVLC can be a promising alternative or complementarity to other UWOC methods for future 5G technology and the achievement of Internet for underwater things.

This work was partially supported by the National Key Research and Development Program of China (No. 2017YFB0403603), National Natural Science Foundation of China (NSFC) (No. 61571133), and Shanghai SHEITC Software and IC Industry Development Project (No. 170326).

References

1. F. Schill, U. R. Zimmer, and J. Trumpf, in *Proceedings of ACRA* (2004), p. 1.
2. N. Chi and M. Shi, Chin. Opt. Lett. **16**, 120603 (2018).
3. N. Chi, Y. Zhao, M. Shi, P. Zou, and X. Lu, Opt. Express **26**, 26700 (2018).
4. G. Cossu, R. Corsini, A. Khalid, S. Balestrino, A. Coppelli, A. Caiti, and E. Ciaramella, in *2013 2nd International Workshop on Optical Wireless Communications (IWOW)* (2013), p. 11.
5. P. Zou, Y. Liu, F. Wang, F. Hu, and N. Chi, Opt. Commun. **438**, 132 (2019).

6. S. Arnon, Opt. Eng. **49**, 015001 (2010).
7. J. Baghdady, K. Miller, K. Morgan, M. Byrd, S. Osler, R. Ragusa, W. Li, B. M. Cochenour, and G. E. Johnson, Opt. Express **24**, 9794 (2016).
8. H. M. Oubei, J. R. Duran, B. Janjua, H.-Y. Wang, C.-T. Tsai, Y.-C. Chi, T. K. Ng, H.-C. Kuo, J.-H. He, and M.-S. Alouini, Opt. Express **23**, 23302 (2015).
9. H. M. Oubei, C. Li, K.-H. Park, T. K. Ng, M.-S. Alouini, and B. S. Ooi, Opt. Express **23**, 20743 (2015).
10. J. Xu, M. Kong, A. Lin, Y. Song, X. Yu, F. Qu, J. Han, and N. Deng, Opt. Commun. **369**, 100 (2016).
11. P. Tian, X. Liu, S. Yi, Y. Huang, S. Zhang, X. Zhou, L. Hu, L. Zheng, and R. Liu, Opt. Express **25**, 1193 (2017).
12. Z. Ghassemlooy, L. N. Alves, S. Zvanovec, and M.-A. Khalighi, *Visible Light Communications: Theory and Applications* (CRC Press, 2017).
13. C. L. Andrews and R. L. Phillips, *Laser Beam Propagation through Random Media* (SPIE Press, 2005).
14. C. Fei, J. Zhang, G. Zhang, Y. Wu, X. Hong, and S. He, J. Lightwave Technol. **36**, 728 (2017).
15. L. Ding, G. T. Zhou, D. R. Morgan, Z. Ma, J. S. Kenney, J. Kim, and C. R. Giardina, IEEE Trans. Commun. **52**, 159 (2004).
16. M. Elamassie, F. Miramirkhani, and M. Uysal, in *2018 IEEE International Conference on Communications Workshops (ICC Workshops)* (2018), p. 1.
17. H. G. Sandalidis, T. Tsiftsis, and G. K. Karagiannidis, J. Lightwave Technol. **27**, 4440 (2009).
18. S. Arnon, Opt. Lett. **28**, 129 (2003).
19. V. J. Mathews and J. Lee, in *International Conference on Acoustics, Speech, and Signal Processing* (1988), p. 1383.
20. J. Shi, Y. Zhou, Y. Xu, J. Zhang, J. Yu, and N. Chi, IEEE Photonics Technol. Lett. **29**, 1183 (2017).
21. J. Zhang, J. Wang, M. Xu, F. Lu, L. Chen, J. Yu, and G.-K. Chang, in *2016 Optical Fiber Communications Conference and Exhibition (OFC)* (2016), p. 1.
22. W. Liu, Z. Xu, and L. Yang, Photonics Res. **3**, 48 (2015).
23. P. A. Haigh, Z. Ghassemlooy, S. Rajbhandari, I. Papakonstantinou, and W. Popoola, J. Lightwave Technol. **32**, 1807 (2014).
24. Y. LeCun, Y. Bengio, and G. Hinton, Nature **521**, 436 (2015).
25. P. L. Bartlett, IEEE Trans. Inf. Theory **44**, 525 (1998).